DOI: 10.24996/ijs.2026.67.11.19

ISSN: 0067-2904

Searching Ground State Properties of ^{22}C, ^{23}Al, and ^{27}P Nuclei Using Whittaker's Wave Functions

Moataz G.Awad*, Arkan R. Ridha
Department of Physics, College of Science, University of Baghdad, Baghdad-Iraq

Received: 20/4/2025 Accepted: 22/2/2026 Published: xx

Abstract

In current work, the Whittaker's wave functions were utilized to search the nuclear ground charge distributions, Coulomb form factors and differential cross sections for some stable nuclei (^{12}C, ^{27}Al, and ^{31}P), besides the density distributions were computed corresponding to them (^{22}C, ^{23}Al, and ^{27}P) as well. The Whittaker's parameters were constrained to produce the available experimental radii. Furthermore, the Whittaker's basis was linked to harmonic-oscillator basis via boundary condition at a specific matching point. For proton-rich nuclei (^{22}C, ^{23}Al, and ^{27}P Nuclei) and stable ^{12}C, the nuclear shell model in pure configuration was opted. For exotic ^{22}C, ^{23}Al and ^{27}P nuclei, the Whittaker's basis was applied exclusively to the final exotic valence proton, unlike the stable ^{12}C, ^{27}Al and ^{31}P which the Whittaker's basis was applied to the last valence proton and neutron. For ^{27}Al and ^{31}P, the mixing configuration was employed using *sd*-shell Bonn A interaction (SDBA) in the sd-shell. In addition to C0 component for ^{31}P, the spin for ^{27}Al is $\frac{5^+}{2}$; there is a C0+C2+C4 component in the empirical Coulomb form factor. The C2 and C4 components were accounted for by applying core-polarization theory within the framework of the Tassie and Bohr-Mottelson models. The model-space contributions to C2+C4 components was calculated using SDBA interaction in the sd-shell. Such approach resulted in very good agreement with experimental measurements.

Keywords: Whittaker's wave function, radioactive nuclei, density distribution, Coulomb form factor, electron scattering differential cross section.

بحث خصائص الحالة الأرضية لنوى ^{22}C, ^{23}Al and ^{27}P باستخدام الدوال الموجية لويتكر

معتز جمعه عواد*, اركان رفعه رضا
قسم الفيزياء، كلية العلوم، جامعة بغداد، بغداد–العراق

الخلاصة

في هذا العمل، تم استخدام دوال ويتكر الموجية للبحث في توزيعات الكثافة النووية في الحالة الأرضية، ومعاملات التشكل الكولومية، ومقاطع التشتت التفاضلية للنوى الغنية بالنيوترونات والبروتونات ونظائرها المستقرة (^{12,22}C, ^{23,27}Al, ^{27,31}P). تم تثبيت معاملات دوال ويتكر لتوليد قيم أنصاف الأقطار العملية المتاحة. تم ربط دوال ويتكر بدوال المتذبذب التوافقي عبر الشرط الحدودية عند نصف قطر القلب. بالنسبة للنوى الغنية

*Email: Motaz.awad2304@sc.uobaghdad.edu.iq

Open Access Articles. This articles is licensed under

بالنيوترونات والبروتونات (^{22}C, ^{23}Al, ^{27}P) والنواة المستقرة ^{12}C تم اعتماد نموذج القشرة النووية بتشككيلات نقية. وبالنسبة للنوى الغريبة (^{22}C, ^{23}Al ^{27}P) تم تطبيق دوال ويتكر فقط على بروتون التكافؤ الخارجي الأخير، على عكس النوى المستقرة (^{31}P, ^{12}C, ^{27}Al) التي تم فيها تطبيق دوال ويتكر على كل من بروتون ونيوترون التكافؤ. بالنسبة للنويتين (^{31}P , ^{27}Al) تم استخدام التشكيلات المختلطة باستخدام تفاعل SDBA في القشرة . *sd* بالإضافة إلى المكون C0 للنواة ^{31}P فإن العزم المغزلي الكلي للنواة ^{27}Al هو $\frac{5}{2}^{+}$ وبالتالي، يوجد مكون C0+C2+C4 في معامل التشكل الكولومي العملي. تم تطبيق نظرية استقطاب النواة لحساب مساهمات C2 و C4 باستخدام نموذجي تاسّي وبور–موتيلسون. تم حساب مساهمة فضاء الانموذج في مكون C2+C4 باستخدام تفاعل SDBA في القشرة *sd* . لوحظ أن مثل هذه المعالجة قد حسنت بشكل كبير الكميات المحسوبة مقارنة بالبيانات ال.

1. Introduction

Radial wave functions are of maximal importance in elucidating nuclear structure, particularly concerning the determination of nuclear sizes and the radial distribution of nucleons within a given nuclear system [1]. Experimental investigations of matter density distributions in exotic nuclei consistently reveal a long-range tail component at larger radii [2]. The electron scattering, the muonic atoms and the optical isotope shift yield significant information concerning the exceedingly minute quantities of radioactive nuclei [3]. Owing to the extremely short lifetimes of halo nuclei, these nuclei are investigated utilizing inverse kinematics [4]; where the role of target and projectile is inverted. Experimental root-mean-square (rms) matter radii are accessible via nucleus-nucleus scattering within the framework of the Glauber model [5,6]. In nuclear calculations, harmonic-oscillator (HO) wave functions are commonly utilized in nuclear density distribution studies due to their analytical tractability. However, their applicability for describing the critical long-range behavior is fundamentally restricted by the inherent Gaussian decay observed at large radial distances (r) [7]. The radial wave functions describing nuclear bound states are characterized by a Gaussian form, transitioning to an exponential decay at asymptotic r region. To address the limitations of harmonic oscillator (HO) wave functions, which inadequately represent the exponential behavior at larger radial distances, alternative potential models or advanced theoretical frameworks are employed. Notably, the Woods-Saxon (WS) potential yields wave functions that more accurately reproduce the observed exponential profile, demonstrating significant utility in the investigation of nuclear states across both stable and unstable isotopes by Gamba et. al., [8]. To address the limitations of standard harmonic oscillator (HO) wave functions, the transformed harmonic oscillator (THO) wave function approach has been developed by Karataglidis and Amos [9]. This methodology has been used by Dhhewy and Ridha for studying the ground state for ^{54}Cr nuclide [10]. Khalaf and Ridha have been successfully applied the HO and spherical Hankel functions to both stable and exotic Flourine isotopes [11]. Finally, Mohammed and Majeed investigated the characteristics of some light mirror nuclei using shell model with acceptable findings [12].

In the current work, to accurately incorporate the contribution of Coulomb interaction of the final proton with the protons of core, Whittaker's wave functions were employed to determine the nuclear ground state characteristics (density distributions and electron scattering form factors) of halo nuclei (^{22}C, ^{23}Al, and ^{27}P) compared with their corresponding stable nuclei (^{12}C, ^{27}Al and ^{31}P).

2.Theory

For any mean field $U(r)$, the radial part of the Schrodinger equation is given by [7]:

$$\left\{-\frac{\hbar^2}{2\mu}\frac{d^2}{dr^2}+\frac{l(l+1)}{2\mu r^2}+U(r)\right\}\phi_{nl,t_z}(r)=E_{nl,t_z}\phi_{nl,t_z}(r) \quad (1)$$

In Eq. (1), the μ represents the reduced mass for the system consisting of core-valence $\left(\mu = \frac{M_c M_v}{M} m_u\right)$, knowing that m_c, M_v and m_u indicate the mass of the core, valence proton and atomic mass unit ($m_u = 931.494\ MeV$) with $M = M_c + M_v$ (total mass of core-valence system), correspondingly. The symbols n, l and t_z stand for the principle quantum number, orbital quantum number and projection of isospin quantum number ($t_z = 1/2$ for proton and $t_z = -1/2$ for neutron). The Coulomb interaction among the final proton(s) with the protons of core, the potential is given by:

$$U(r) = \frac{1}{4\pi\varepsilon_0}\frac{Z_c Z_v}{r} \tag{2}$$

The Z_c and Z_v are the number of protons in the core and valence, correspondingly.
After substituting Eq. (2) into Eq. (1) one yields:

$$\left\{\frac{d^2}{dr^2} - \frac{l(l+1)}{r^2} - 2\frac{\eta k}{r} - k^2\right\}\phi_{nl,t_z}(r) = E_{nl,t_z}\phi_{nl,t_z}(r) \tag{3}$$

The solution to Eq. (3), is given by [14]:

$$\phi_{nl,t_z}(r) = C_{nl,t_z} W_{-\eta,l+\frac{1}{2}}(2kr) \tag{4}$$

Via the continuity of WF at a specific match point, the constant C_{nl,t_z} in Eq. (4) can be found.

In Eqs. (3) and (4), the η, is a unitless parameter called Somerfield's parameter computed from:

$$\eta = \frac{Z_1 Z_2 e^2 \mu}{\hbar^2 k} \tag{5}$$

The k is the wave number and it is given in the unit of fm^{-1}:

$$k = \sqrt{\frac{2\mu E}{\hbar^2}} \tag{6}$$

where $\hbar c = 197.329\ MeV.fm$.
At matching point (R_c), the continuity of WF of the final halo proton can be written as:

$$u_1(R_c) = u_2(R_c) \tag{7}$$

Where:

$$u_1(r) = R_{nl}(r), \quad harmonic - oscillator\ WF \tag{8}$$

and

$$u_2(r) = C_{nl,t_z}\frac{W_{-\eta,l+\frac{1}{2}}(2kr)}{r} \quad (Whittaker\ WF\ ) \tag{9}$$

Therefore, Eq. (7) can be simplified to:

$$R_{nl}(R_c) = C_{nl,t_z}\frac{W_{-\eta,l+\frac{1}{2}}(2kR_c)}{R_c} \tag{10}$$

The WF of the interior and exterior can be written as:

$$R_{nl}^{mod}(r) = \begin{cases} R_{nl}(r), & 0 < r \le R_c \\ C_{nl,t_z}\frac{W_{-\eta,l+\frac{1}{2}}(r)}{r}, & R_c < r \le \infty \end{cases} \tag{11}$$

The normalized form to Eq. (11), $N_{nl}^2 \int_0^\infty \left|R_{nl}^{mod}(r)\right|^2 r^2 dr = 1$ can be written as:

$$N_{nl}^2\left[\int_0^{R_c} |R_{nl}(r)|^2 r^2 dr + C_{nl,t_z}^2 \int_{R_c}^{\infty} \left|W_{-\eta,l+\frac{1}{2}}(r)\right|^2 dr\right] = 1 \tag{12}$$

or

$$N_{nl}^2[I_{interior} + I_{exterior}] = 1 \tag{13}$$

Finally, Eq. (13) can be detailed to:

$$\bar{R}_{nl}^{mod}(r) = N_{nl}\begin{cases} R_{nl}(r), & 0 < r \le R_c \\ C_{nl,t_z}\frac{W_{-\eta,l+\frac{1}{2}}(r)}{r}, & R_c < r \le \infty \end{cases} \tag{14}$$

Besides, the probability of the valence proton(s) inside (P_{in}) and outside (P_{out}) core (R_c) can be found as:

$$P_{in} = N_{nl}^2 I_{interior}, \quad 0 < r \le R_c \tag{15}$$

$$P_{out} = N_{nl}^2 I_{exterior}, \quad R_c < r \le \infty \tag{16}$$

The neutron and proton distributions for proton-rich and stable nuclei are given correspondingly as:

$$\rho_{t_z=-\frac{1}{2}}(r) = \frac{1}{4\pi}\sum_{n,l\in core} occ\#_{nl,t_z=-\frac{1}{2}}|R_{nl}(r)|^2 + \frac{1}{4\pi}\left|\bar{R}_{nl}^{mod}(r)\right|^2 \tag{17}$$

$$\rho_{t_z=\frac{1}{2}}(r) = \frac{1}{4\pi}\sum_{n,l\in core} occ\#_{nl,t_z=\frac{1}{2}}|R_{nl}(r)|^2 + \frac{1}{4\pi}\sum_{n,l\in valence} occ\#_{nl,t_z=\frac{1}{2}}\left|\bar{R}_{nl}^{mod}(r)\right|^2 \tag{18}$$

The matter distribution is computed from:

$$\rho_m(r) = \rho_{t_z=\frac{1}{2}}(r) + \rho_{t_z=-\frac{1}{2}}(r) \tag{19}$$

where $occ\#_{nl,t_z}$ represents the proton (neutron) number in the orbit a inside the core (a stands for n and l quantum numbers). The charge density distribution (CDD) is accounted from the folding integration procedure outlined by Elton [14] and Chandra [15]:

$$\rho_{ch,t_z=1/2}(r) = \int \rho_{J=0,t_z=1/2}(r)\rho_{pr}(\boldsymbol{r}-\boldsymbol{r'})d\boldsymbol{r'} \tag{20}$$

$$\rho_{ch,t_z=-1/2}(r) = \int \rho_{J=0,t_z=-1/2}(r)\rho_{neu}(\boldsymbol{r}-\boldsymbol{r'})d\boldsymbol{r'} \tag{21}$$

The rms radius was accounted from [15]:

$$\sqrt{< r^2 >_i} = \sqrt{\frac{4\pi}{i}\int_0^\infty \rho_i\,(r)r^4 dr} \tag{22}$$

The i in Eq. (22) indicates the protons, neutrons, charge and nucleons.

In the plane-wave Born approximation, the Coulomb form factors for electron scattering involving multipolarity J are given by:

$$F_{ch}^J(q) = \frac{4\pi}{Z}\int_0^\infty j_J(qr)\rho_{charge,J}(r)r^2 dr \tag{23}$$

Where:

$$\rho_{ch,J}(r) = \rho_{ch,J}^{CP}(r) + \rho_{ch,J}^{MS}(r) \tag{24}$$

The Z in Eq. (23) stands for the atomic number, $j_J(qr)$ is the spherical Bessel function and q represents the momentum transferred to target nucleus from incident electrons.

Besides, in Eq. (23), the $\rho_{ch,J}(r)$ is branched into two parts; one for the core (or the core-polarization (CP) contribution) and the second is the model space. For the core contribution, two mathematical forms of CP were opted; the first one is the Tassie model [16] and the second is the Bohr-Mottelson model [17], both given respectively by:

$$\rho_{charge,J}^{CP}(r) = N_T r^{J-1}\frac{d}{dr}\rho_{charge}(r) \tag{25}$$

$$\rho^{CP}_{charge,J}(r) = N_{BM}\frac{d}{dr}\rho_{charge}(r) \quad (26)$$

The contribution of model space is given by [16]:

$$\rho^{MS}_{J,t_z}(r) = \frac{1}{\sqrt{4\pi}}\frac{1}{\sqrt{2J_i+1}}\sum_{ab} X^{J_f\ J_i\ J}_{a,b,t_z}\ \langle j_a||Y_J||j_b\rangle\ R_{n_a l_a j_a,t_z}(r)R_{n_b l_b j_b,t_z}(r) \quad (27)$$

The constants, N_T and N_{BM} in Eqs. (25) and (26) were opted to produce the experimental quadrupole moments:

$$N_T = \frac{\sqrt{(2J_i+1)B(CJ,J_i\rightarrow J_f)-\int_0^\infty r^{J+2}\rho^{MS}_{J,ch}(r)dr}}{\int_0^\infty r^{2J+1}\frac{d\rho_{ch}(r)}{dr}dr} \quad (28)$$

$$N_{BM} = \frac{\sqrt{(2J_i+1)B(CJ,J_i\rightarrow J_f)-\int_0^\infty r^{J+2}\rho^{MS}_{J,ch}(r)dr}}{\int_0^\infty r^{J+1}\frac{d\rho_{ch}(r)}{dr}dr} \quad (29)$$

where $J_i = J_f = J$ for elastic transition, besides, the reduced transition probability is proportional to the experimental quadrupole moment as:

$$B(CJ,J\rightarrow J) = \frac{5Q^2_{exp.}}{16\pi(2J_i+1)\begin{pmatrix} J & 2 & J \\ -J & 0 & J\end{pmatrix}^2} \quad (30)$$

3.Results and discussion

This study investigates the properties of ground state for ^{12,22}C, ^{23,27}Al, and ^{27,31}P. The calculations of rms radii, density distributions, and Coulomb form factors were performed using the Whittaker's (W) wave functions (WF). The shell model in pure configuration was harnessed to all investigated proton-rich nuclei with stable ^{12}C. In contrast, the configuration mixing was utilized to perform the calculations for stable ^{27}Al and ^{31}P, employing the sd-shell Bonn A interaction (SDBA) [18]. The theoretical computations of one-body density matrix elements (OBDMEs) were performed using the nuclear shell model code *Nushell* [19].

Table 1 presents a summary of the properties of the searched proton-rich nuclei (^{23}Al and ^{27}P) in parallel with the Borromean nucleus ^{22}C (proton-rich nucleus); the overall initial spin and parity (J_i^π), the overall initial isospin (T_i), the half–life time ($t_{1/2}$), the size parameter of HO (b_c) for nucleons in core, the radius of core (r_c), the Somerfield parameter (η_p), the wave number (k_p), the quantum numbers of HO and W (n, l), and the final single–particle separation energy ($E_p\ or E_n$).

Table 2 presents the computed size radii for ^{22}C (Borromean nucleus), ^{23}Al, and ^{27}P, utilizing the parameters of the harmonic oscillator (HO) and Whittaker potentials detailed in Table 1. These computed values are subsequently compared with corresponding experimental data.

Table 3 tabulates the probabilities of the last halo proton(s) residing within (P_{in}) and outside (P_{out}) the core radius r_c. The presented results indicate that the P_{out} values for the studied halo proton-rich nuclei are significantly greater than, or approximately equal to 50%, P_{in}, thereby confirming their halo nature. For ^{27}P nucleus, our theoretical calculations supporting the presence of proton skin.

Table 4 presents the same as in Table 1 but for the studied stable nuclei (^{12}C, ^{27}Al and ^{31}P).

Table 5 presents the same as in Table 2 for the calculated size radii but for stable ^{12}C, ^{27}Al and ^{31}P.

Figure 1 displays the calculated matter distributions for ^{22}C, ^{23}Al, and ^{27}P (the solid curves are the calculations of Whittaker (W) potential) alongside with experimental data (represented by shaded areas and dotted curves). For ^{22}C, ^{23}Al, and ^{27}P a very good match is evident among the experimental data and the theoretical predictions derived from the HO+W (harmonic-oscillator plus Whittaker). The extended tail, which is a key signature of halo nuclei, is highly bred by the theoretical calculations. Besides, in Figure 1 (a), the gray solid curve represents the calculated proton density distribution compared with experimental dotted grey symbols.

Figure 2 presents the calculated charge density distributions (CDDs) for stable ^{12}C, ^{27}Al and ^{31}P denoted by solid curves (which are represented by Whittaker). Experimental data are indicated by dotted curves. A clear congruence is observed among the computed CDDs and the experimental values.

In Figure 3, the computed charge form factors (C0) for stable ^{12}C and ^{31}P only. C0+C2+C4 for ^{27}Al nucleus was displayed and compared with experimental values. For ^{12}C, ^{27}Al and ^{31}P the calculated C0 form factors (solid curves represented by HO+W) are in good agreement with experimental data (represented by triangles black and gray). Regarding ^{27}Al, the $J_i^\pi = J_f^\pi = \frac{5^+}{2}$ (see Table 4) which gives the multipolarities $J = 2$ and $J = 4$ (from selection rule: $|J_i - J_f| \leq J \leq J_i + J_f$). The experimental charge form factor is C0+C2+C4, therefore, C2+C4 components were incorporated in our calculations using two theoretical models; the Tassie model (T) denoted by black curve and Bohr-Mottelson model (BM) denoted by gray curve. From Eq. (24), the CDD is branched into two parts one for the core and the second is for model space. The core contribution is accounted using Eqs. (25) and (26). The model-space contribution was accounted using Eq. (27). The constants of normalization in Eqs (28) and (29) were opted to generate the experimental quadrupole moment for ^{27}Al; $Q_{exp.} = 14.02\ e.fm^2$ [20]. For the full sd −shell model-space, the SDBA interaction [18] was adopted. The shell model calculations were fulfilled using the *Nushell* code [19]. It is clear that the theoretical findings using BM and T are in very good match with experimental values. For stable ^{27}Al $\left(J^\pi = \frac{5^+}{2}\right)$ and ^{31}P $\left(J^\pi = \frac{1^+}{2}\right)$ [22], the occupation numbers predicted by the nuclear shell model calculations using SDBA interaction [18] where the core of such interaction is ^{16}O; $\left(n_{\pi 1s_{\frac{1}{2}}}\right) = 2.$, $\left(n_{\pi 1p}\right) = 6.$, $\left(n_{\nu 1s_{\frac{1}{2}}}\right) = 2.$, $\left(n_{\nu 1p}\right) = 6.$ are: For ^{27}Al: $\left(n_{\pi 1d_{\frac{5}{2}}}\right) \approx 3.167$, $\left(n_{\pi 1d_{\frac{3}{2}}}\right) \approx 1.114$, $\left(n_{\pi 2s_{\frac{1}{2}}}\right) \approx 0.717$, $\left(n_{\nu 1d_{\frac{5}{2}}}\right) \approx 3.440$, $\left(n_{\nu 1d_{\frac{3}{2}}}\right) \approx 1.210$, $\left(n_{\nu 2s_{\frac{1}{2}}}\right) \approx 1.349$. For ^{31}P: $\left(n_{\pi 1d_{\frac{5}{2}}}\right) \approx 4.167$, $\left(n_{\pi 1d_{\frac{3}{2}}}\right) \approx 1.578$, $\left(n_{\pi 2s_{\frac{1}{2}}}\right) \approx 1.254$, $\left(n_{\nu 1d_{\frac{5}{2}}}\right) \approx 4.417$, $\left(n_{\nu 1d_{\frac{3}{2}}}\right) \approx 2.183$, $\left(n_{\nu 2s_{\frac{1}{2}}}\right) \approx 1.399$.

In Figure 4, the calculated differential cross section was depicted for ^{12}C, ^{27}Al and ^{31}P. The dotted symbols represent experimental values. The solid curves represent the calculated differential cross sections (which denoted by HO+W). The theoretical differential cross sections were computed for incident energies of values: 374.5 MeV and 747 MeV for ^{12}C, 250 MeV and 400 MeV for ^{31}P, 250 MeV and 400 MeV for ^{27}Al. In general, It is obvious that the calculations were in good match with experimental values.

Table 1: The ground-state characteristics and Whittaker's parameters for ^{22}C, ^{23}Al, and ^{27}P nuclei.

${}^{A}_{Z}X_{N}$ $(J^\pi\ T)$ [21]	$t_{1/2}(s)$ [21]	$b_{c,p}(fm)$	$b_{c,n}(fm)$	r_c	η_p	k_p (fm^{-1})	n,l	$Cal.$ $S_p\ or\ S_n(MeV)$
${}^{22}_{6}C_{16}(0^+0)$	$6.2ms$	2.1	2.195	4	0	0.0418	$2s1/2$	0.02
${}^{23}_{13}Al_{10}\left(\frac{5^+}{2}\ \frac{3}{2}\right)$	$470\ ms$	1.864	1.666	3.3	4.941	0.0806	$2s1/2$	0.141
${}^{27}_{15}P_{12}\left(\frac{1^+}{2}\ \frac{3}{2}\right)$	$260ms$	2.344	2.12	5.5	2.328	0.2009	$2s1/2$	0.870

Table 2: The computed and available size radii for ^{22}C, ^{23}Al, and ^{27}P nuclei.

${}^{A}_{Z}X_{N}$	$Cal.$ $< r^2 >^{1/2}_{ch}$	Exp $< r^2 >^{1/2}_{ch}$	Cal. $< r^2 >^{1/2}_{p}$	Exp $< r^2 >^{1/2}_{p}$	Cal. $< r^2 >^{1/2}_{n}$	Exp $< r^2 >^{1/2}_{n}$	Cal. $< r^2 >^{1/2}_{m}$	Exp $< r^2 >^{1/2}_{m}$
${}^{22}_{6}C_{16}$	3.151	–	3.090	-	4.999	5.0(0.8) [25]	5.345	5.4(0.9)
${}^{23}_{13}Al_{10}$	3.182	-	3.099	3.1(0.25) [23]	2.633	2.634(0.23 [23]	2.906	2.905(0.25) [23]
${}^{27}_{15}P_{12}$	3.455	-	3.379	3.38(0.26) [24]	2.997	3.00(0.17) [24]	3.215	3.22(0.23) [24]

Table 3: The probabilities inside (P_{in}) and outside (P_{out}) the r_c of the last halo proton for ^{22}C, ^{23}Al, and ^{27}P nuclei.

${}^{A}_{Z}X_{N}$	P_{in}	P_{out}
${}^{22}_{6}C_{16}$	16.36%	83.71%
${}^{23}_{13}Al_{10}$	37.31%	62.21%
${}^{27}_{15}P_{12}$	74.20%	25.81%

Table 4: The ground-state characteristics and Whittaker's parameters for ^{12}C, ^{27}Al and ^{31}P.

${}^{A}_{Z}X_{N}$ $(J^{\pi}\ T)$ [21]	$b_{c,p}$ (fm)	$b_{c,n}$ (fm)	η_p	η_n	k_p (fm^{-1})	k_n (fm^{-1})	n,l	r_c (fm)	$Exp.$ $E_n(MeV)$	$Exp.$ $E_p(MeV)$
${}^{12}_{6}C_{6}(0\ 1^{+})$	1.663	1.685	0.189	0	0.839	0.910	$1p_{3/2}$	2	18.720	15.956
${}^{27}_{13}Al_{14}\left(\frac{5^{+}}{2}\ \frac{1^{+}}{2}\right)$	1.837	1.84	0.752	0	0.652	0.853	$1d_{3/2}$	2.8	13.058	8.271
${}^{31}_{15}P_{16}\left(\frac{1^{+}}{2}\ \frac{1}{2}\right)$	1.892	1.92	1.516	0	0.725	1.097	$2s_{1/2}$	3	12.311	7.296

Table 5: Computed and experimental charge, proton, neutron, matter *rms* radii for ^{12}C, ^{27}Al, and ^{31}P nuclei.

${}^{A}_{Z}X_{N}$	Cal. $< r^2 >^{1/2}_{ch}$	Exp. $< r^2 >^{1/2}_{ch}$ [22]	Cal. $< r^2 >^{1/2}_{p}$	Cal. $< r^2 >^{1/2}_{n}$	Exp. $< r^{2>1/2}_{n}$ [25]	Cal. $< r^2 >^{1/2}_{m}$	Exp. $< r^{2>1/2}_{m}$ [25]
${}^{12}_{6}C_{6}$	2.463	2.464(12)	2.356	2.383	–	2.369	–
${}^{27}_{13}Al_{14}$	3.06	3.05(5)	2.975	3.009	-	2.993	-
${}^{31}_{15}P_{16}$	3.189	3.187(11)	3.108	3.149	-	3.130	-

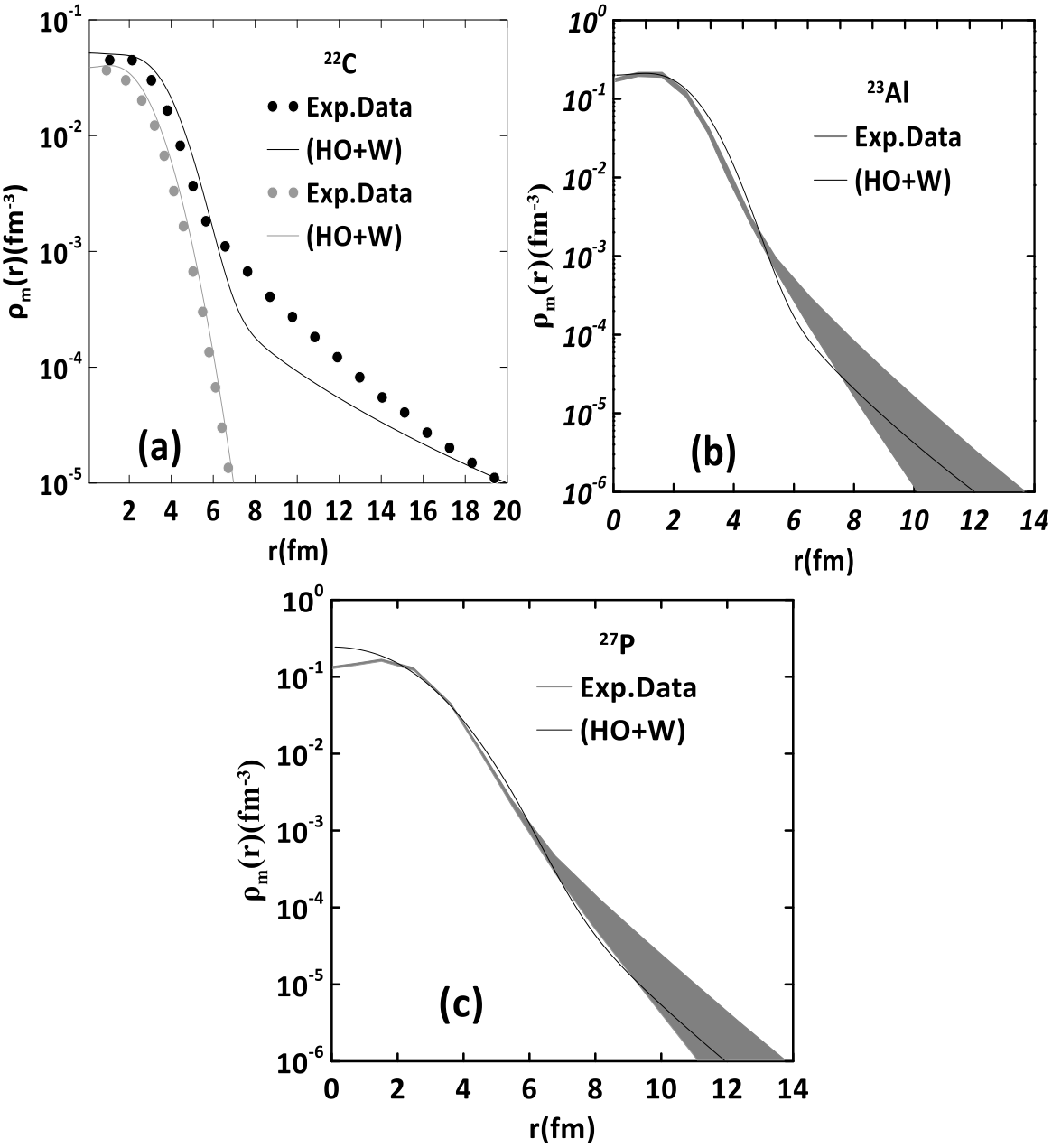


Figure 1: The calculated and experimental matter distributions for ^{22}C(a) [25] ,^{23}Al(b) [23] and ^{27}P(c) [26].

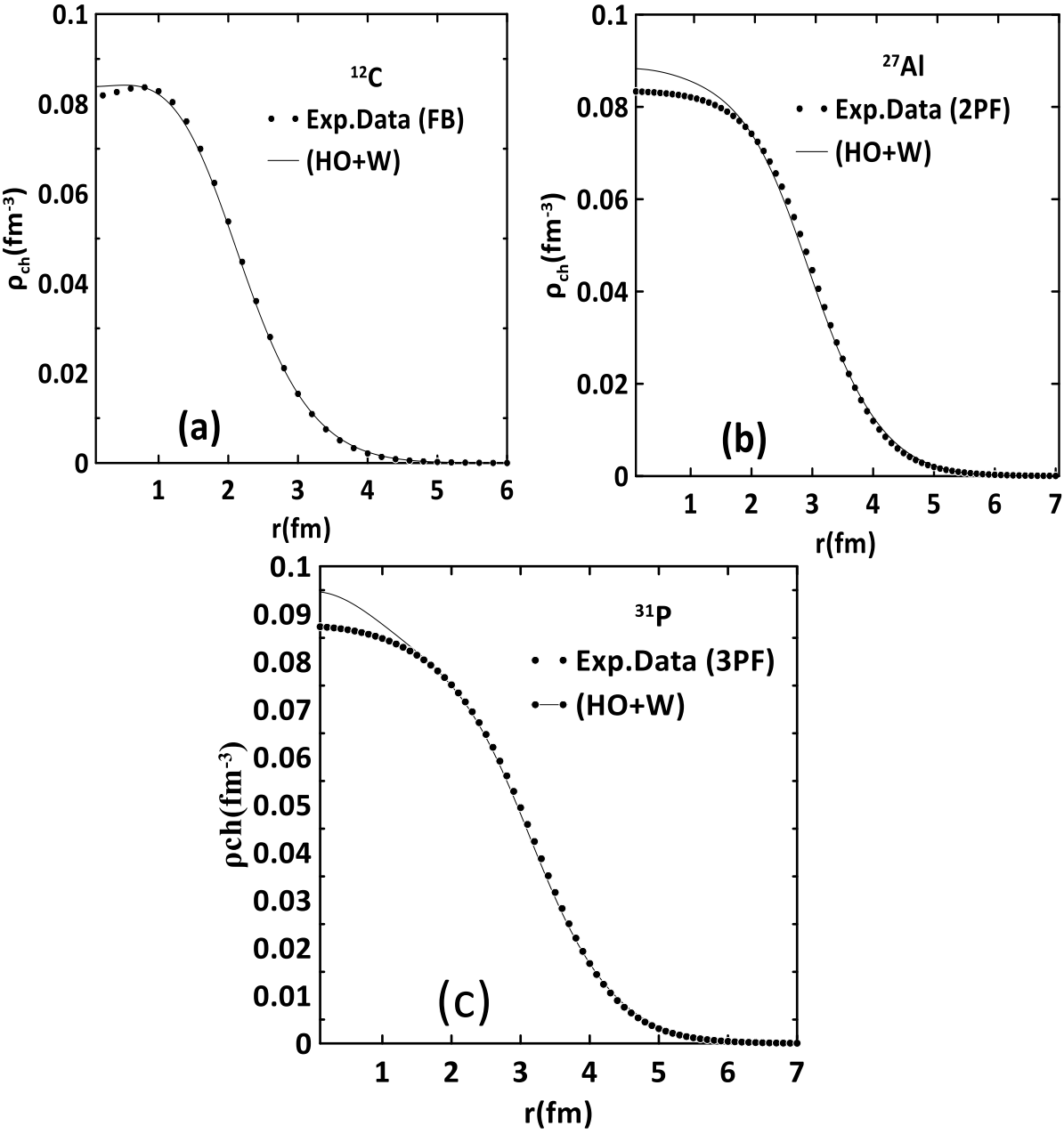


Figure 2: The computed and experimental CDDs for ^{12}C(a),^{27}Al(b) and ^{31}P(c). the model independent using Fourier-Bessel (FB), two-parameter Fermi (2PF) and three-parameter Fermi (3PF) were used [22].

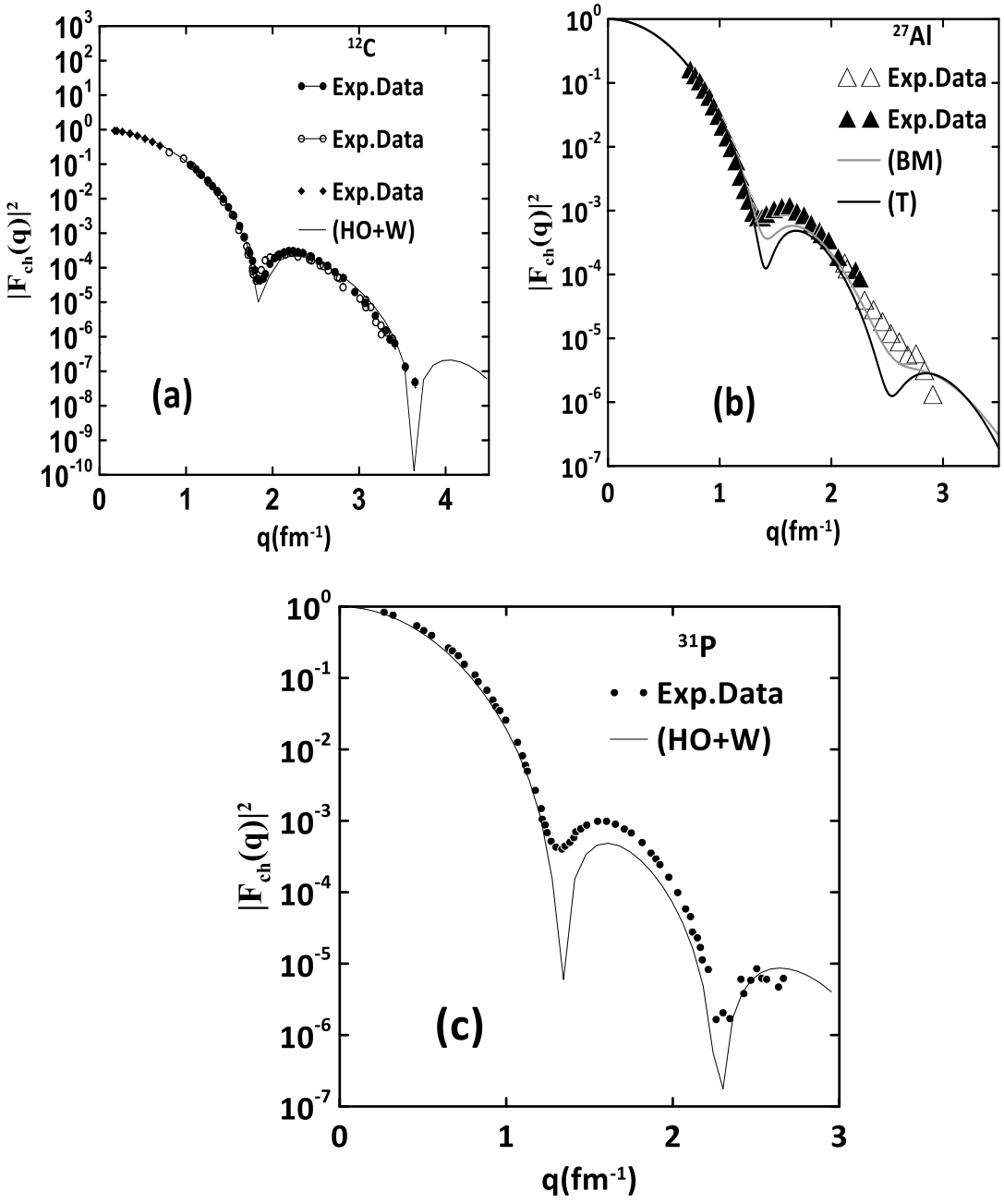


Figure 3: The calculated and experimental charge form factors for ^{12}C(a) [27], ^{27}Al(b) [28] and ^{31}P(c) [29].

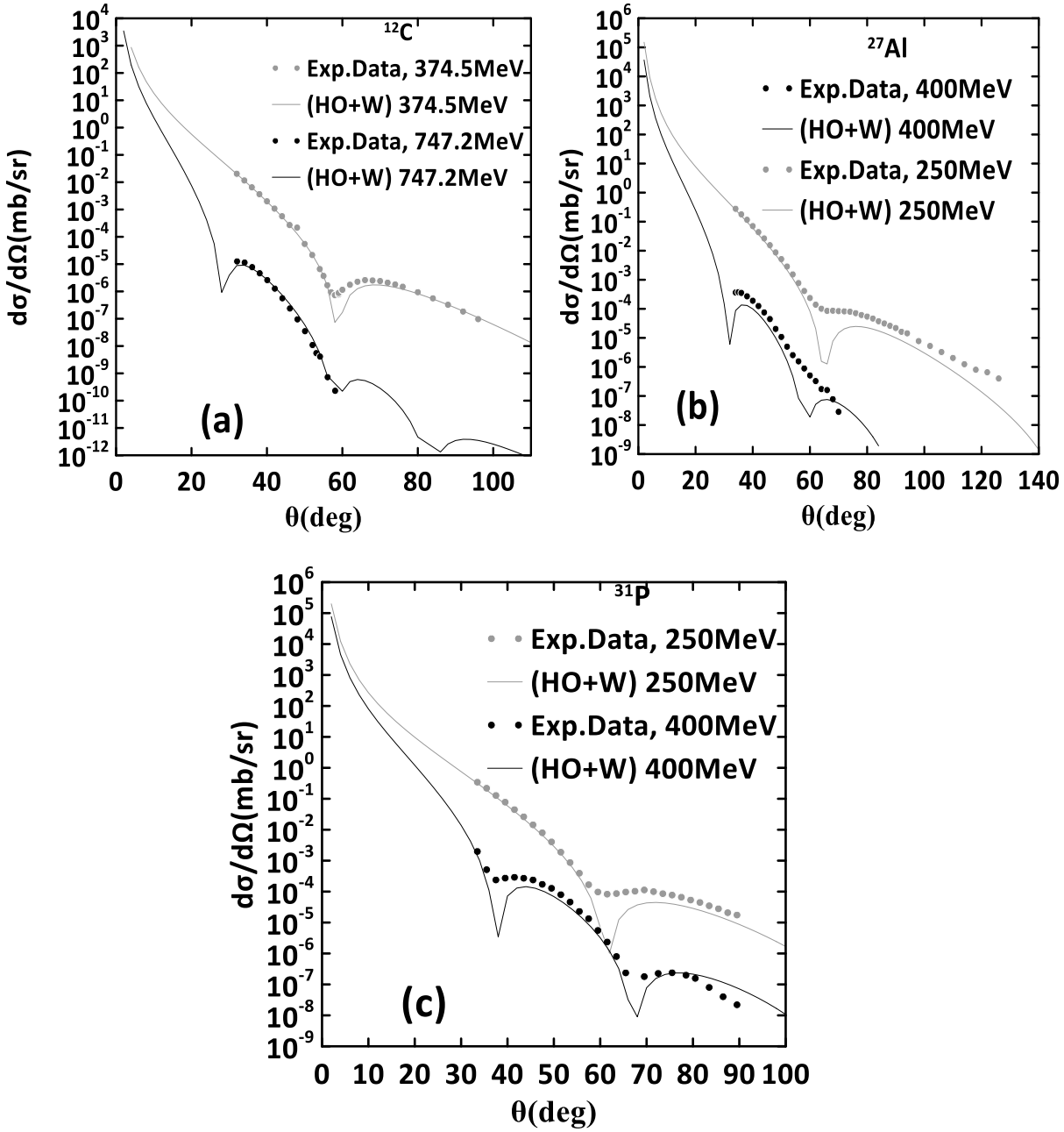


Figure 4: The computed and experimental cross section for ^{12}C(a) [27] ,^{27}Al(b) [30] and ^{31}P(c) [29].

4.Conclusions

In this study, it is concluded that the use of Whittaker basis provides a highly effective approach for searching the bulk characteristics; density distributions (for ^{22}C, ^{23}Al, and ^{27}P nuclei) and charge form factors for the investigated stable nuclei (^{12}C, ^{27}Al, and ^{31}P). Good match was obtained among theoretical and experimental data. The independent-particle model was employed for all searched nuclei. Regarding the halo nuclei under investigation ^{22}C, ^{23}Al and ^{27}P, Whittaker's wave functions effectively reproduced the long tail characteristic in the asymptotic region, demonstrating a good agreement with experimental data. The theoretical findings suggest that a reduction in the binding energy of the outermost valence proton(s) results in an expansion of the nuclear tail region. For the calculated charge density distributions for the stable nuclei (^{12}C, ^{27}Al and ^{31}P), the theoretical predictions demonstrated good match with experimental data. Furthermore, for ^{27}Al, the C2 and C4 Coulomb form factors were computed

incorporating core polarization effects, utilizing both the Bohr-Mottelson and Tassie models, alongside with the inclusion of model space considerations by the SDBA interaction in the full sd −shell. The results obtained from the Bohr-Mottelson (B-M) and Tassie models demonstrated a good match with the experimental data for C0+C2+C4 data.

References

[1] C. J. Batty, E. Friedman, H. J. Gils, and H. Rebel, "Experimental Methods for Studying Nuclear Density Distributions," *Adv. Nucl. Phys.*, no. 19, pp. 1–188, 1989, doi: 10.1007/978-1-4613-9907-0_1.

[2] I. Tanihata, H. Savajols, and R. Kanungo, "Recent experimental progress in nuclear halo structure studies," *Prog. Part. Nucl. Phys.*, vol. 68, no. 1, pp. 215–313, 2013, doi: 10.1016/j.ppnp.2012.07.001.

[3] C. A. Bertulani, "*Nuclear Physics in a Nutshell*," 1st Edition. Princeton, USA. Princeton University Press, 2007.

[4] I. Tanihata, "Neutron halo nuclei," *J. Phys. G Nucl. Part. Phys.*, vol. 22, no. 2, pp. 157–198, Feb. 1996, doi: 10.1088/0954-3899/22/2/004.

[5] I. Tanihata, et al "Measurements of interaction cross sections and radii of He isotopes," *Phys. Lett. B*, vol. 160, pp. 380-384., 1985.

[6] A. Ozawa, T. Suzuki, and I. Tanihata, "Nuclear size and related topics," *Nucl. Phys. A*, vol. 693, no. 1–2, pp. 32–62, 2001, doi: 10.1016/S0375-9474(01)01152-6.

[7] K. L. G. Heyde, "*The Nuclear Shell Model*", Study Edition. Berlin, Heidelberg, New

a. York. Springer-Verlag, 1994.

[8] S. Gamba, G. Ricco, and G. Rottigni, "A phenomenological Woods-Saxon potential for p-shell nuclei," *Nucl. Physics, A*, vol. 213, no. 2, pp. 383–396, 1973, doi: 10.1016/0375-9474(73)90159-0.

[9] S. Karataglidis, K. Amos, and B. G. Giraud, "Local scale transformations and extended matter distributions in nuclei," *Phys. Rev. C* ., vol. 71, no. 6, pp. 1–24, 2005, doi: 10.1103/PhysRevC.71.064601.

[10] M. M. Dhhewy and A. R. Ridha, "Searching Elastic and Inelastic Coulomb Transitions in Chromium-54 ," *Passer J. Basic Appl. Sci.*, vol. 7, no. 1, pp. 204–210, 2025.

[11] S. A. J. Khalaf and A. R. Ridha, "Properties of Ground-State of ^{17,19,20,24,26}F using the Wave Functions of Harmonic-Oscillator and Spherical Hankel Functions," *Iraqi J. Sci.*, vol. 64, no. 2, pp. 668–675, 2023, doi: 10.24996/ijs.2023.64.2.16

[12] R. A. Mohammed and W. Z. Majeed, "Exotic Structure of ^{17}Ne-^{17}N and ^{23}Al-^{23}Ne Mirror Nuclei," *East Eur. J. Phys.*, no. 4, pp. 72–79, 2022, doi: 10.26565/2312-4334-2022-4-05.

[13] M. Abramowitz and I.A. Stegun, "*Handbook of Mathematical Functions with Formulas, Graphs, and Mathematical Tables* , " (Applied Mathematics Series). Washington, DC, USA: National Bureau of Standards, 1964.

[14] L. R. B. Elton, "*Nuclear Sizes*", London, UK. Oxford University Press, 1961.

[15] H.Chandra and G.sauer, "Relativistic corrections to the elastic electron scattering from ^{208}Pb," *Phys. Rev. C*, vol. 13, no. 1, pp. 245–252, 1975, doi: 10.1103/PhysRevC.13.245.

[16] G. Bertsch and S. F. Tsai, "How good is the collective model?," *Phys. Lett. B*, vol. 50, no. 3, pp. 319–322, 1974, doi: 10.1016/0370-2693(74) 90679-0.

[17] A. N. Bohr and B. R. Mottelson, "*Nuclear Structure,* " Vol. 1.: *Single-Particle Motion*, Singapore. World Scientific Publishing Company, 1998.

[18] B. A. Brown and W. A. Richter, "New 'USD' Hamiltonians for the sd shell," *Phys. Rev. C* vol. 74, no. 3, pp. 1–11, 2006, doi: 10.1103/PhysRevC.74.034315.

[19] B. A. Brown and W. D. M. Rae, "Nushell @ MSU, MSU-NSCL report," pp. 1–34, 2007.

[20] N. J. Stone, "Table of nuclear magnetic dipole and electric quadrupole moments,." *Nucl. Data Tables*, vol .90, no.1, pp.75-176,2005, doi: 10.1016/j.adt.2005.04.001.

[21] G. Audi, F. G. Kondev, M. Wang, W. J. Huang, and S. Naimi, "The NUBASE2016 evaluation of nuclear properties .," *Chinese Phys. C*, vol. 41, no. 3, 2017, doi: 10.1088/1674-1137/41/3/030001.

[22] H. De Vries, C. W. De Jager, and C. De Vries, "Nuclear charge-density-distribution parameters from elastic electron scattering," *At. Data Nucl. Data Tables*, vol. 36, no. 3, pp. 495–536, 1987,

doi: 10.1016/0092-640X(87)90013-1.

[23] H.Y. Zhang, et al "Measurement of reaction cross section for proton-rich nuclei (A < 30) at intermediate energies," *Nucl. Phys. A*, vol. 707, no. 3–4, pp. 303–324, 2002, doi: 10.1016/S0375-9474(02)01007-2.

[24] D.Q. Fang, et al "Evidence for a proton halo in ^{27}P through measurements of reaction cross-sections at intermediate energies," *Eur. Phys. J. A*, vol. 12, no. 3, pp. 335–339, 2001, doi: 10.1007/s100500170011.

[25] K. Tanaka, et al "Observation of a large reaction cross section in the drip-line nucleus ^{22}C," *Phys. Rev. Lett.*, vol. 104, no. 6, pp. 10–13, 2010, doi:10.1103/PhysRevLett.104.062701.

[26] W. Q. Shen, et al "Measurements of total reaction cross sections for neutron-deficient nuclei (A<30) and investigation on possible proton halo nuclei," pp. 658–662, 2007, doi: 10.1063/1.1470010.

[27] I. Sick and J. S. McCarthy, "Elastic electron scattering from ^{12}C and ^{16}O," *Nucl. Phys. A*, vol. 150, no. 3, pp. 631–654, 1970, doi : 10.1016/0375-9474(70)90423-9.

[28] P. P. Singhal, A. Watt, and R. R. Whitehead, "Elastic electron scattering from ^{23}Na, ^{25}Mg and ^{27}Al and a shell-model interpretation," *J. Phys. G Nucl. Phys.*, vol. 8, no. 8, pp. 1059–1083, 1982, doi: 10.1088/0305-4616/8/8/012.

[29] B. B. P. Sinha and G. A. Peterson, G. C. Li and R. R. Whitney "Nuclear Charge Distributions of Isotone Pairs. I. ^{31}P and ^{32}S," *Phys. Rev. C*, vol. 6, no. 5, pp. 1657–1663, 1972, doi:10.1103/PhysRevC.6.1657.

[30] G. C. Li, M. R. Yearian, and I. Sick, "High-momentum-transfer electron scattering from ^{24}Mg, ^{27}Al, ^{28}Si, and ^{32}S," *Phys. Rev. C*, vol. 9, no. 5, pp. 1861–1877, 1974, doi: 10.1103/PhysRevC.9.1861.